Further investigation of perturbations in FLRW space-time

P. R. Dhungel*, S. K. Sharma** and U. Khanal***

*Department of Physics, St. Xavier's College, Tribhuvan University, Kathmandu, Nepal.

**B.P. Koirala Memorial Planetarium, Observatory and Science Museum Development Board, MoEST, Kathmandu, Nepal.

***Professor of Physics, Mid-Baneshwor, Kathmandu, Nepal.

Abstract: The solutions of perturbation equations in FLRW spacetime were further analysed for indications of structure formation. The radial and angular parts of the wavefunction reveal various possibilities of spatial and angular sizes in terms of quantum numbers ω, k, l and m. They offer slightly contrasting results for the three cases of the closed, open and flat universes including for each of all the 3 modes of perturbations – scalar, vectorial and tensorial. It is seen that the structures of large scales are more compact in the closed case, slightly diffuse in the flat one. Also structures of different sizes are more probable in the open case.

Keywords: FLRW space-time; Perturbation; Large-scale structure; NP formalism.

Introduction

How the large-scale structures (LSS) are formed in the universe is one of the crucial questions that the cosmologists have been working on for a long time. The formation of LSS begins with small density fluctuations seeded in the early universe, imprinted during cosmic inflation. These fluctuations arise from quantum fluctuations magnified to macroscopic scales during the rapid expansion of the universe[1, 2]. So, perturbation analysis provides a powerful framework for studying the formation and evolution of LSS in the universe, helping cosmologists to understand the underlying physics and test theoretical models against observational data[3].

Perturbation analysis in the context of Friedmann-Lemaitre-Robertson-Walker (FLRW) spacetime, which describes the homogeneous and isotropic universe on large scales, faces several challenges and open problems including understanding the behaviour of perturbations in the nonlinear regime[4], incorporating the effects of dark energy and dark matter accurately[5], improving our understanding of the initial conditions for density fluctuations[6, 7], developing robust methods for analysing observational data and extracting cosmological information[8], and even extending the perturbation theory to alternative theories of gravity[9, 10].

Progress in perturbation analysis in FLRW spacetime is essential for advancing our understanding of the universe's large-scale structure and testing fundamental theories of cosmology and gravity. That's why the perturbations in FLRW spacetime have been further investigated in this paper extending authors' previous work[11]. Neumann-Penrose (NP) formalism[12] has been successfully applied to derive perturbation equations and find their solutions in 3 different modes namely tensorial, vectorial and scalar.

For all the three cases of closed, flat and open universe, curvature constant K = 1, 0 and -1 respectively, the angular part Y is always the spin weighted spherical harmonic with spin-weight $|p|=0$, for scalar (density), 1 for vectorial (rotational) and 2 for tensorial (gravitational) perturbations. The radial part R can be solved in terms of a boost-weight

functions that looks almost like the spin-weighted angular part, but in terms of non-conventional Jacobi polynomials that are nonetheless orthogonal. They can be analytically continued into the open case, and reduce to Coulomb wave functions in the flat one[13]. So we have been canvassing for an integrated view of the three cases, the over-density regions as closed universe, voids as open and the near region as flat part of the Universe.

In terms of Jacobi polynomials[14], $P_n^{(\alpha,\beta)}$, the angular and spatial parts are given respectively as

$$_pY_l^m = Ne^{im\phi}(1-\cos\theta)^{\frac{m+p}{2}}(1+\cos\theta)^{\frac{m-p}{2}}P_{l-m}^{(m+p,\ m-p)}(\cos\theta) \quad \ldots(1)$$

$$_pR_k^\omega = \ _pN_k^\omega(1-i\cot r)^{-\frac{(\omega+p)}{2}}(1+\cot r)^{-\frac{(\omega-p)}{2}}P_{\omega-k-1}^{(-\omega-p,-\omega+p)}(i\cot r) \quad \ldots(2)$$

where, the spin helicity p takes the values ± 2 for tensorial perturbations, ± 1 for vectorial perturbations and 0 for scalar perturbations; N is normalization constant; the parameters of Jacobi Polynomials are chosen such that the function will be regular at r = 0 and π.

Further analysis are done in the next section.

Analysing the solutions of perturbation equations

For the case of closed universe (*i.e.*,K = 1), the angular and radial parts of the wavefunction, $\psi = YR$, are given by equations (1) and (2). Some 3D plots of $|\Psi|^2$ for various cases are shown in Fig. 1.

For the flat case (*i.e.*, K = 0), the equation for the radial eigenfunction comes to be in the form of Coulomb wave equation[13]

$$R''(r) + \left(\omega^2 - \frac{2i\omega p}{r} - \frac{k(k+1)}{r^2}\right)R(r) = 0 \quad \ldots(3)$$

It's solutions are in terms of Confluent Hypergeometric[15] function M(a, b, z) given by

$$R_k(ip, \omega r) = C_l(ip)(\omega r)^{k+1}e^{\mp\omega r}M(k+1\pm p, 2k+2, 2i\omega r) \quad \ldots(4)$$

where, the normalizing constant

$$C_l(ip) = \frac{2^l e^{-2\pi p/2}|\Gamma(k+1-p)|}{(2k+1)!} \quad \ldots(5)$$

Some typical plots of $|R|^2$ for various values of ω, k and l for all the three modes – tensorial, vectorial and scalar have been shown in Fig 2. The corresponding 3D plots have been shown in Fig. 3.

Tensorial Perturbation (p = 2), for w = 3, k=2, m=2, l=2

Tensorial Perturbation (p = 2), for w = 5, k=4, m=2, l=3

Vectorial Perturbation (p = 1), for w = 3, k=2, m=2, l=2

Vectorial Perturbation (p = 1), for w = 5, k=4, m=2, l=3
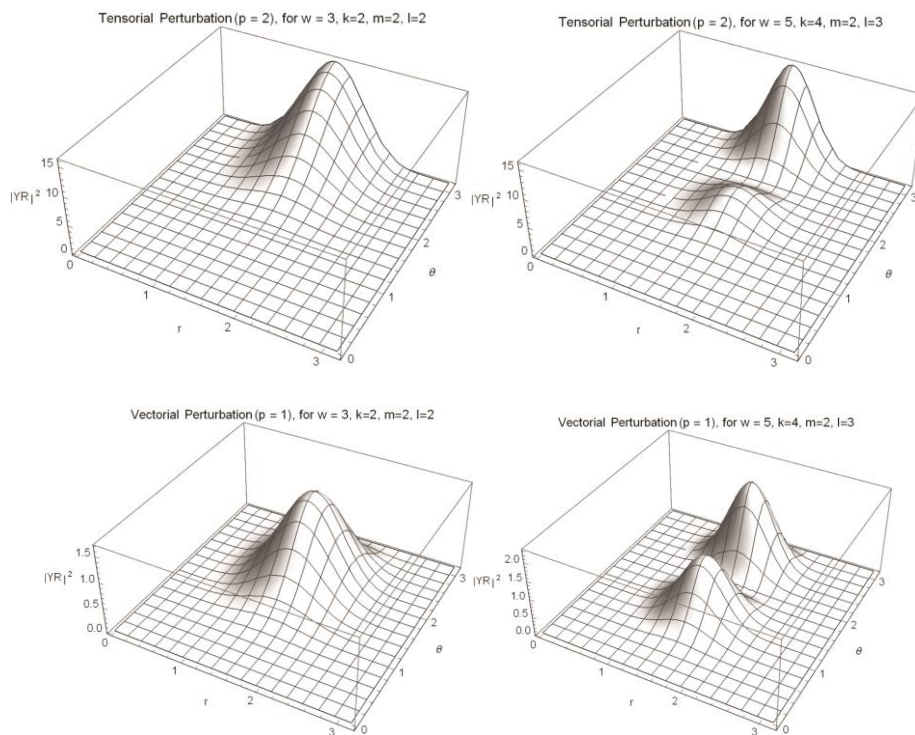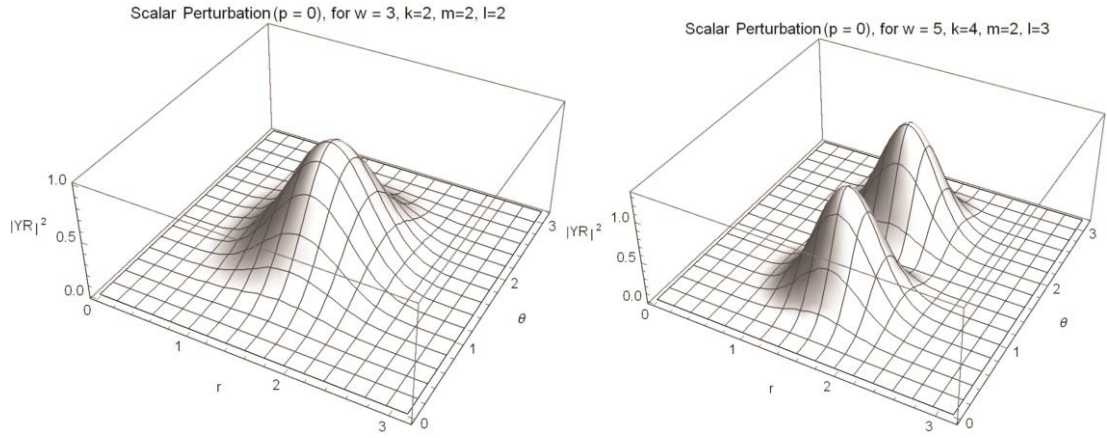
Fig.-1: 3D plots of $|YR|^2$ against r and θ for Tensorial (top), vectorial (middle) and scalar (bottom) perturbations for the closed universe. The left ones are for $\omega = 3, k = 2, l = 2, m = 2$ and on the right are for $\omega = 5, k = 4, l = 3, m = 2.$

For the case of open universe (*i.e.*, K = -1), the radial part R of the solution is similar to the one for the closed case given by Eq. (2) with trigonometric function replaced by hyperbolic function:

$$_pR_k^\omega = \quad _pN_k^\omega(1 - i\ coth\ r\ )^{-\frac{(\omega+p)}{2}}(1 +$$

$$coth\ r\ )^{-\frac{(\omega-p)}{2}}P_{\omega-k-1}^{(-\omega-p,-\omega+p)}(i\ coth\ r\ ) \quad ...(6)$$

The angular part Y remains same as for the closed one given by Eq. (1). The 3D plots of $|YR|^2$ are shown in Fig. 4.
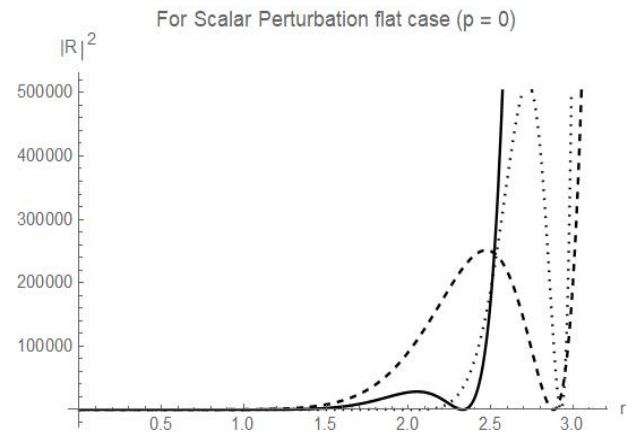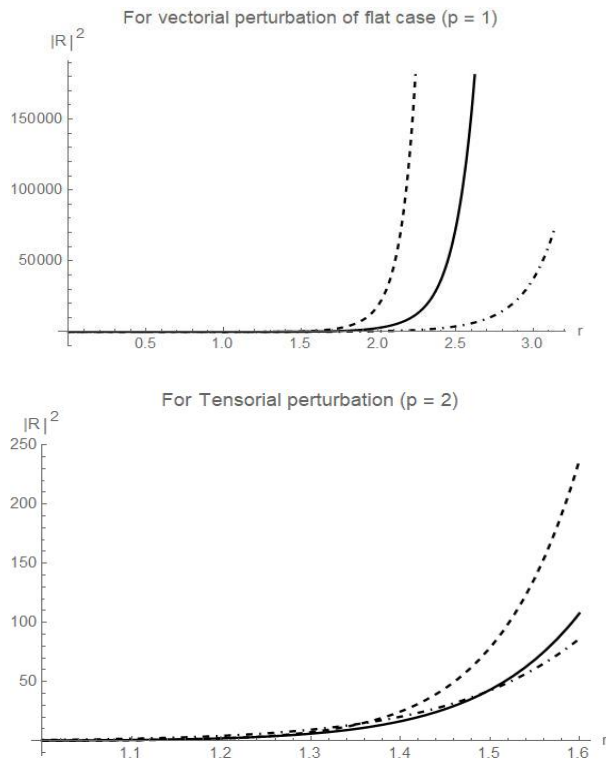
Fig.-2: Plots of $|R|^2$ against r for scalar(bottom), vectorial (middle) and tensorial (top) perturbations for flat case. The dashed curve is for $\omega = k = 2$, solid curve is for $\omega = k = 3$ and dot-dashed one is for $\omega = k = 4$. All are for $l = 1$. The first ones are scaled differently in order to bring to comparable sizes.

In all the three cases, structure formation is seen to be more probable in large scales. Further discussion is in the next section.

Discussion and Conclusions

In order to have insights into the physics of large scale structure formation, we have further investigated the perturbations. The peaking of the perturbation amplitude at large values of r as seen explicitly in Fig.1 shows that the structures of large-scales are easily formed in the case of closed universe. The flat portion of the graph for smaller sizes suggests that there is little power or amplitude in the density perturbations at those scales. This could imply the presence of a characteristic scale below which density
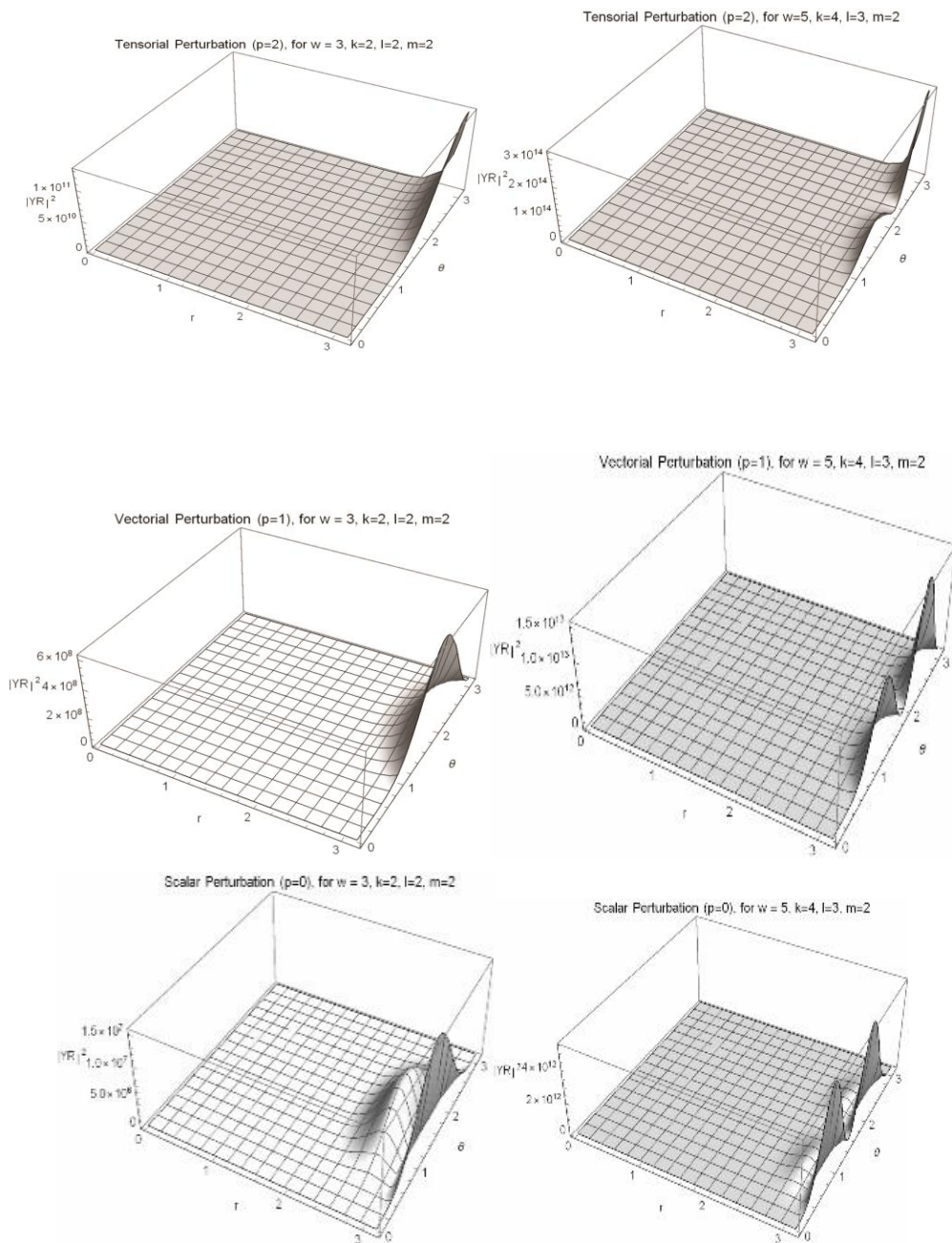
Fig.-3: 3D plots of |YR|² against r and θ for scalar (bottom), vectorial (middle) and tensorial (top) perturbations for flat case. Those on the left are for ω = 3, $k = m = l = 2$ and those on the right are for ω = 5, $k = 4, l = 3, m = 2$.

fluctuations are suppressed or inhibited. This scale may be related to physical processes such as baryon acoustic oscillations (BAO) or the damping effects of free-streaming particles like neutrinos.

The zoomed portions of typical plots of the closed case for a narrow range of r and θ show the separation between two clusters or galaxies. Obtaining its order of magnitude of these separations in order to be able to correlate them with the observed BAO scales[16] will be taken up in future work.
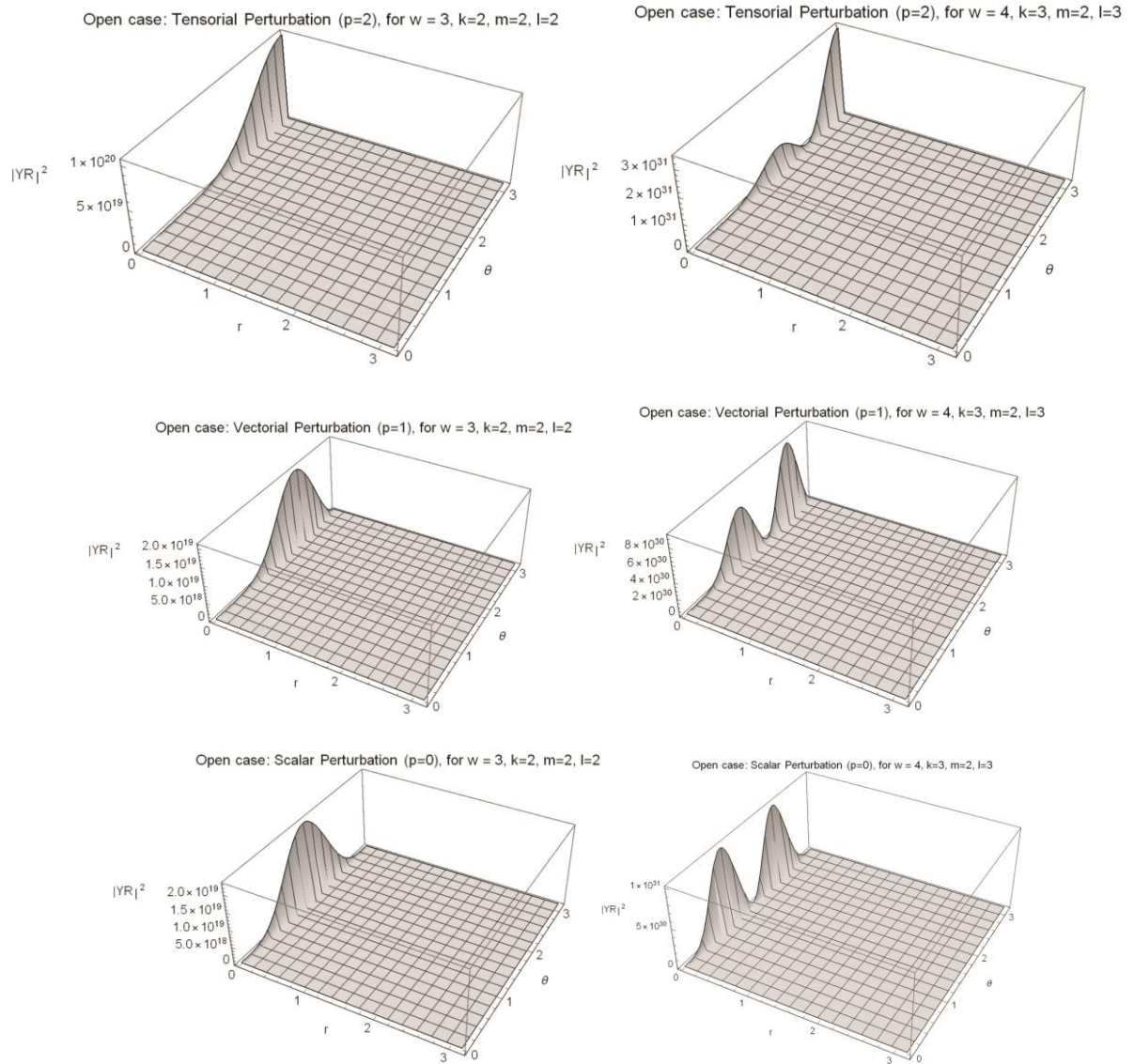
Fig.-4: 3D plots of $|YR|^2$ against r and θ for scalar (bottom), vectorial (middle) and tensorial (top) perturbations for open case. Those on the left are for ω = 3, $k = m = l = 2$ and those on the right are for ω = 5, $k = 4$, $l = 3$, $m = 2$.

As shown in Fig. 2 and 3, in the flat case also, the structures of larger scales are more probable to form. However, the smaller perturbations have also been seen to grow. In the closed case (as shown in Fig. 4), the compact structures of various scales seem to be possible to be formed.

Although the power spectrum has been and widely used tool for analysing large-scale structure in cosmology nowadays[17], the method of directly analysing the perturbation wavefunction that we have used like the one in this paper has the advantages in terms of providing detailed spatial information, capturing nonlinear effects, specifying initial conditions, accessing higher-order statistics, facilitating observational modelling, and enabling a deeper physical interpretation of the underlying processes. These will be extended in future works.

References

1. Peebles, P. J. E. 1980. The large-scale structure of the universe. *Princeton University Press.*

2. Weinberg, S. 1972. Gravitation and cosmology: principles and applications of the general theory of relativity. *John Wiley & Sons.*

3. Coles, P. and Lucchin, F. 2002. Cosmology: The origin and evolution of cosmic structure. *Wiley-Blackwell.*

4. Bernardeau, F., Colombi, S., Gaztañaga, E. and Scoccimarro, R. 2002. Large scale structure of the universe and cosmological perturbation theory. *Physics Reports*. **367**(1-3): 1-248.

5. Linder, E. V. 2003. Exploring the expansion history of the universe. *Physical Review Letters*. **90**(9): 091301.

6. Komatsu, E., et al. 2011. Seven-year Wilkinson Microwave Anisotropy Probe (WMAP) observations: cosmological interpretation. *The Astrophysical Journal Supplement Series*. **192**(2): 18.

7. Planck Collaboration. 2018. Planck 2018 results. VI. Cosmological parameters. *Astronomy & Astrophysics*. 641: A6.

8. Alam, S., et al. 2017. The clustering of galaxies in the completed SDSS-III baryon oscillation spectroscopic survey: cosmological analysis of the DR12 galaxy sample. *Monthly Notices of the Royal Astronomical Society*. **470**(3): 2617-2652.

9. Clifton, T., Ferreira, P. G., Padilla, A. and Skordis, C. 2012. Modified gravity and cosmology. *Physics Reports*. **513**(1-3): 1-189.

10. Joyce, A., Jain, B., Khoury, J. and Trodden, M. (2015). "Beyond the cosmological standard model". *Physics Reports*. 586:1-98.

11. Sharma, S. K. and Khanal, U. 2014. Perturbation of FRW spacetime in NP formalism. *Int. J. Mod. Phys.* D 23 : 1450017.

12. Neumann, E. T. and Penrose, R. 1962. J. *Math. Phys.* **3**: 566.
https://dlmf.nist.gov/33.2, cited on 15 March 2024.

13. Gradshteyn, I. S. and Ryzhik, I. M. 1980. Table of Integral, Series and Products. *Academic, New York*.

14. Abramowitz, M. and Stegun, I. A. 1976. Handbook of Mathematical Functions. *Dover, New York*.

15. Percival, W.J. et al., 2010. Baryon acoustic oscillations in the sloan digital sky survey data release 7 galaxy Sample. *Monthly Notices of the Royal Astronomical Society*. **401** (4): 2148-2168.

16. Halle, A., et al., 2010. Power spectrum response of large-scale structure in 1D and in 3D: tests of prescriptions for post-collapse dynamics. *Monthly Notices of the Royal Astronomical Society*. **499** (2): 1769-1787.